



National  
Defence

Défense  
nationale

AD-A261 981



**A NEW ANALYSIS OF THE  
MULTIPATH RADAR DATA MEASURED BY  
STANDARD TELECOMMUNICATION LABORATORIES**

by

**Eric K.L. Hung, Robert W. Herring  
and Janet E. Morris**

DTIC

SELECTED  
MAR 24 1993

E

D

**DEFENCE RESEARCH ESTABLISHMENT OTTAWA**  
REPORT NO. 1138

**DISTRIBUTION STATEMENT**

Approved for public release  
Distribution Unlimited

Canada

December 1992  
wa

93 3 23 051

93-06021





National  
Defence

Défense  
nationale

# **A NEW ANALYSIS OF THE MULTIPATH RADAR DATA MEASURED BY STANDARD TELECOMMUNICATION LABORATORIES**

by

**Eric K.L. Hung**  
*Surface Radar Section  
Radar Division*

and

**Robert W. Herring**  
*Defence Research Establishment Suffield  
Medicine Hat, Alberta, Canada*

and

**Janet E. Morris**  
*AIT Corporation  
Nepean, Ontario, Canada*

**DEFENCE RESEARCH ESTABLISHMENT OTTAWA**  
REPORT NO. 1138

PCN  
041LC

December 1992  
Ottawa

## ABSTRACT

Presented is a new analysis of some multipath radar data measured by Standard Telecommunication Laboratories (STL) Ltd, using an array antenna and low-flying aircraft. The data have previously been analyzed with the singular value decomposition (SVD) method by Haykin, Greenlay, and Litva. These authors were mainly interested in whether or not the SVD method produced target elevation estimates consistently close to an optical track. The new analysis, also using the SVD method, has produced additional results. Firstly, it demonstrates a practical technique for selecting target elevation estimates when the target range was less than 6.5 km. Secondly, it provides an explanation, supported with simulations, for the presence of many false tracks branching out from the target and image tracks.

## RESUME

Ce rapport présente une nouvelle analyse de données radar concernant le phénomène de trajets multiples. Ces données, obtenues avec une antenne réseau et un véhicule aérien volant à basse altitude, ont été analysées par Haykin, Greenlay et Litva à l'aide de la méthode de Décomposition en Valeurs Singulières (DVS). Ces auteurs s'intéressaient principalement à savoir si la méthode DVS produisait des estimés de l'élévation de la cible qui collaient sans exception à une piste optique. La nouvelle technique présentée ici utilise aussi la méthode DVS mais apporte des résultats additionnels. En premier lieu, ce rapport démontre une technique pratique pour la sélection des estimés de l'élévation de la cible quand la distance de celle-ci est inférieure à 6.5 Km. En second lieu, ce rapport fournit une explication, appuyée par des simulations, de la présence de plusieurs fausses pistes sortant de la piste de la cible et de celle de l'image.

iii

DTIC QUALITY INSPECTED 1

Accession For	
NTIS CRA&I	<input checked="checked" type="checkbox"/>
DTIC TAB	<input type="checkbox"/>
Unannounced	<input type="checkbox"/>
Justification	
By	
Distribution/	
Availability Codes	
Dist	Avail and/or Special
A-1	

## EXECUTIVE SUMMARY

This report contains a new analysis of the low-angle tracking radar data measured by Standard Telecommunications Laboratories in the summer of 1981. The radar was an X-band array antenna located at the Fraser Gunnery Range near Portsmouth, United Kingdom. The targets were Hunter and Canberra aircraft flying low over the English Channel. An optical tracker, mounted close to the receive array, provided an independent measure of the target elevation.

The data have previously been analyzed by Haykin, Greenlay, and Litva. They studied whether or not the SVD method produced target elevation estimates consistently close to the optical track. In the study, these estimates were identified as the candidate signal elevation estimates closest to the optical tracks.

The analysis was very limited in scope. Besides, it did not account for the fact that the SVD method produces more candidate signal elevation estimates than other direction-finding methods.

This new analysis is concerned with the development of a practical method for selecting target elevation estimates. It also studies all the candidate signal elevation estimates generated by the SVD method. The results show that (a) the optical track need not be known in the selection of the target elevation estimates, if the target range was less than 6.5 km, (b) there are many false tracks branching out from the true target and image tracks, and (c) target and image tracks with these branches can be generated by adding calibration phase errors to uncorrupted data.

## TABLE OF CONTENTS

	<u>PAGE</u>
ABSTRACT/RESUME	iii
EXECUTIVE SUMMARY	v
TABLE OF CONTENTS	vii
LIST OF FIGURES	ix
1.0 INTRODUCTION	1
2.0 MULTIPATH RADAR DATA	2
3.0 ELEVATION ESTIMATES CALCULATED WITH THE STL DATA	3
3.1 Calculation of signal Elevation Estimates	3
3.2 Results and Observations	3
4.0 EFFECT OF CALIBRATION PHASE ERRORS ON ELEVATION ESTIMATES	11
5.0 CONCLUSIONS	17
6.0 ACKNOWLEDGEMENT	18
7.0 REFERENCES	19
8.0 APPENDIX - CALCULATION OF ELEVATION ESTIMATES	20

## LIST OF FIGURES

- Figure 1      Signal elevation estimates calculated with the singular value decomposition method and the first STL data file. The solid line is derived from the optical tracker output.
- Figure 2      Signal elevation estimates calculated with the singular value decomposition method and the second STL data file.
- Figure 3      Signal elevation estimates calculated with the singular value decomposition method and the third STL data file.
- Figure 4      Signal elevation estimates calculated with the singular value decomposition method and the fourth STL data file.
- Figure 5      Signal elevation estimates calculated with the singular value decomposition method and the fifth STL data file.
- Figure 6      The larger of the two signal elevation estimates derived from the first STL data file.
- Figure 7      Candidate signal elevation estimates derived from simulated data. SNR for 10 km target range is 20 dB.
- Figure 8      Candidate signal elevation estimates derived from the simulated data used in Fig. 7. Table 1 for calibration phase errors applied.
- Figure 9      Candidate signal elevation estimates derived from the simulated data used in Fig. 7. The calibration phase errors are the negative of those in Table 1.
- Figure 10     Signal elevation estimates derived from simulated data. SNR for 10 km target range is 6 dB. Table 1 has been applied to the data.

## 1.0 INTRODUCTION

The multipath radar data in this analysis were obtained by Pearson and Waddoup [1] of Standard Telecommunication Laboratories (STL) Ltd with a vertically oriented X-band array antenna. The targets were aircraft flying low over the English Channel. An optical tracker mounted close to the antenna provided an independent measure of the aircraft elevation.

A previous analysis of these data, using the Tufts-Kumaresan singular value decomposition (SVD) method [2,3], has been reported by Haykin, Greenlay, and Litva [4]. The primary question addressed was whether or not the SVD method consistently produced target elevation estimates close to the true target elevation. These authors identified the candidate signal elevation estimates closest to the optical track as the target elevation estimates.

This new analysis of the STL data is concerned with the development of a practical method for selecting target elevation estimates. It also studies all the candidate signal elevation estimates generated by the SVD method. The results show that the optical track need not be known in the selection of the target elevation estimates, if the target range was less than 6.5 km. They also reveal the presence of many false tracks branching out from the target and image tracks. A possible reason, supported by computer simulations, for these tracks is given.

The presentation is organized as follows. Initially, the multipath radar data are briefly described in Section II. Next, the target elevation estimates calculated with the SVD method are discussed in Section III. The presence of false tracks is noted, and a technique to select target elevation estimates derived. Then, computer simulations are presented in Section IV to demonstrate that false tracks branching out from the target and image tracks can be generated by adding array calibration phase errors to uncorrupted simulated data. Finally, some concluding remarks are given in Section V.

## 2.0 MULTIPATH RADAR DATA

The multipath radar data were measured by STL in 1981 at the Fraser Gunnery Range near Portsmouth, United Kingdom. Separate vertically polarized transmit and receive antennas were used. The transmitter operated at a frequency of 9.6 GHz, corresponding to a wavelength of 3.125 cm. The receive antenna was a vertically oriented, uniform, linear array comprising eight sectorial H-plane horns stacked on top of each other. The height of each horn was 12.50 cm, thus giving an element spacing of 4.0 wavelengths, an antenna aperture of 100 cm, and a beamwidth of 1.79 degrees in the boresight direction. An optical tracker was mounted near the receive antenna to provide an independent measure of the target elevation.

We have access to five data files. The first two were measured on the morning of 18th June, 1981, with a Hunter aircraft flying towards the receive antenna at a nominal altitude of 46 m. The height of the antenna centre was 6.7 m above water. The other three files were measured on the afternoon of 25th June with a Canberra aircraft at an altitude of 61 m. The corresponding height of the antenna centre was 7.9 m. A calibration table, measured on July 2 with a nearfield source, was provided.

It was noted in [1] that there were date-dependent offsets in the optical tracker output and antenna boresight directions, and that these offsets would result in radar elevation errors equal to 0.141 and 0.169 beamwidths for the data collected on June 18 and 25, respectively. There were also uncertainties in the horizontal reference direction for the optical tracker, and this tracker had been readjusted before the data measurement on June 25.

Further details on the experiments appear in [1] and [4].



### 3.0 ELEVATION ESTIMATES CALCULATED WITH THE STL DATA

We describe the calculation of target and image elevation estimates, and then present the results and observations.

#### 3.1 Calculation of Signal Elevation Estimates

The calibration table is applied to the array snapshots in the multipath radar data. Each snapshot is then used in a two-step procedure to calculate two signal elevation estimates. Firstly, the root variant of the SVD method is used to calculate a set of six candidate signal elevation estimates from the snapshot, using  $K=6$  for the filter order and  $M=2$  for the number of signals present. Secondly, the power associated with each candidate signal elevation estimate is calculated and the two strongest estimates are identified as signal elevation estimates. The details of these two steps are given in the appendix.

The filter order is calculated with the relation  $K=3N/4$ , where  $N$  is the number of array elements. This relation is recommended by Tufts and Kumaresan in [2]. The choice of  $M=2$  for the number of signals present follows [4], where the best results were obtained with this number.

#### 3.2 Results and Observations

The two signal elevation estimates (because  $M=2$ ) from each array snapshot in the five STL files are plotted as individual dots in Figs. 1 to 5. No attempts are made to link them, or to associate a dot with the aircraft, the aircraft's image, or a false estimate. The solid lines in the figures are derived from the optical tracker outputs.

There are several observations. Firstly, the dots show a distinct tendency to form patterns strongly suggestive of an output "target" track close to the optical track and an output "image" track below the horizontal direction. Secondly, many false tracks branch out from the target and image tracks. They sometimes link the target and image tracks together. Examples of linkages are clearly visible at ranges 3.4, 4.2 and 6.5 km in Fig. 5. Thirdly, the output target tracks are biased. The biases, or the distances above the optical tracks, are about 0.15 and 0.10 beamwidths for the data collected on June 18 and June 25, respectively.

Fig. 6, derived from the first STL file, is typical of the new results obtained when only the signal elevation estimate with

the higher elevation is plotted. Below 6.5 km, the estimates form an output track close to the optical track. Based on this observation, a target elevation estimate can be obtained from an array snapshot in three steps: calculate a set of six candidate elevation estimates with the snapshot; find the two with the highest power; and pick the one with the higher elevation. This procedure is more practical than the one in [4], because an optical track is usually unavailable.

The bias in output target elevation estimates confirms the presence of offsets in the optical tracker output and antenna boresight directions. It is date-dependent, because the optical tracker had been readjusted before STL files 3 to 5 were measured on June 25.

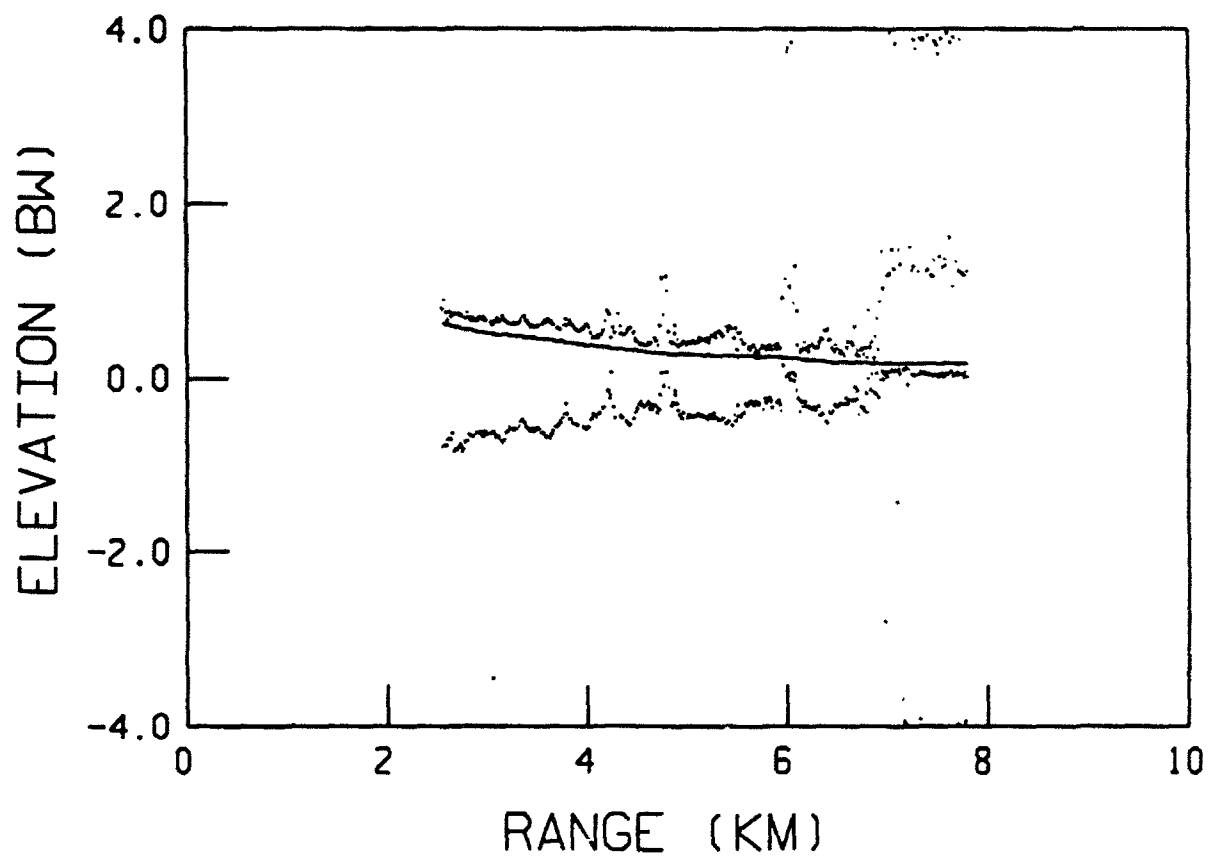


Fig. 1 Signal elevation estimates calculated with the singular value decomposition method and the first STL data file. The solid line is derived from the optical tracker output.

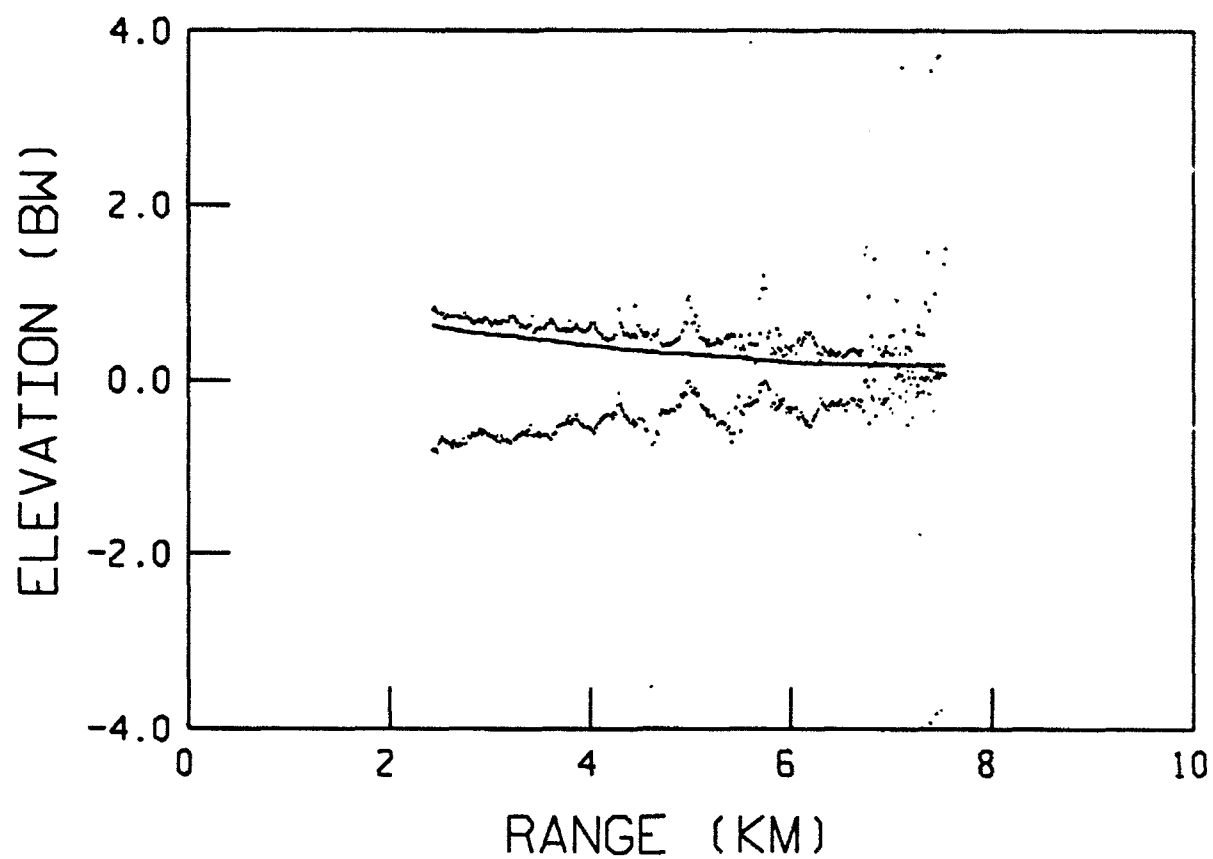


Fig. 2 Signal elevation estimates calculated with the singular value decomposition method and the second STL data file.

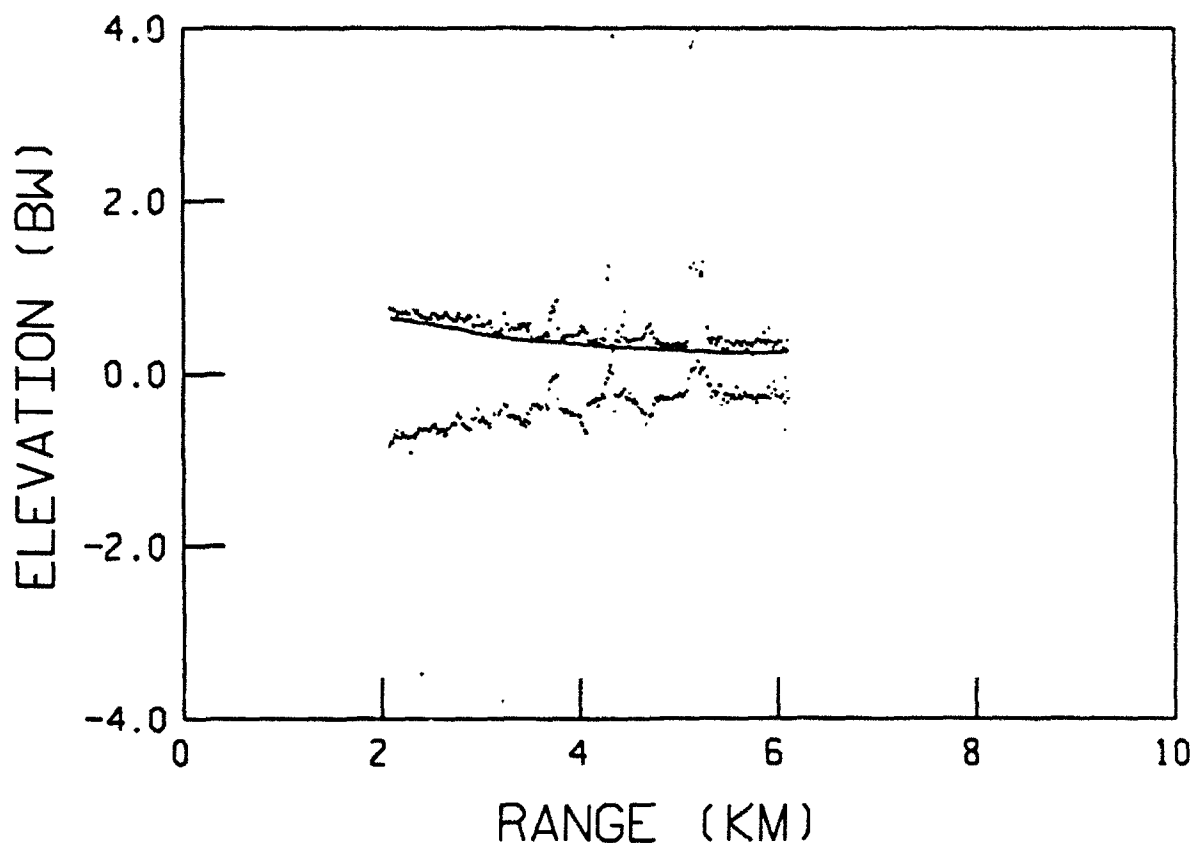


Fig. 3 Signal elevation estimates calculated with the singular value decomposition method and the third STL data file.

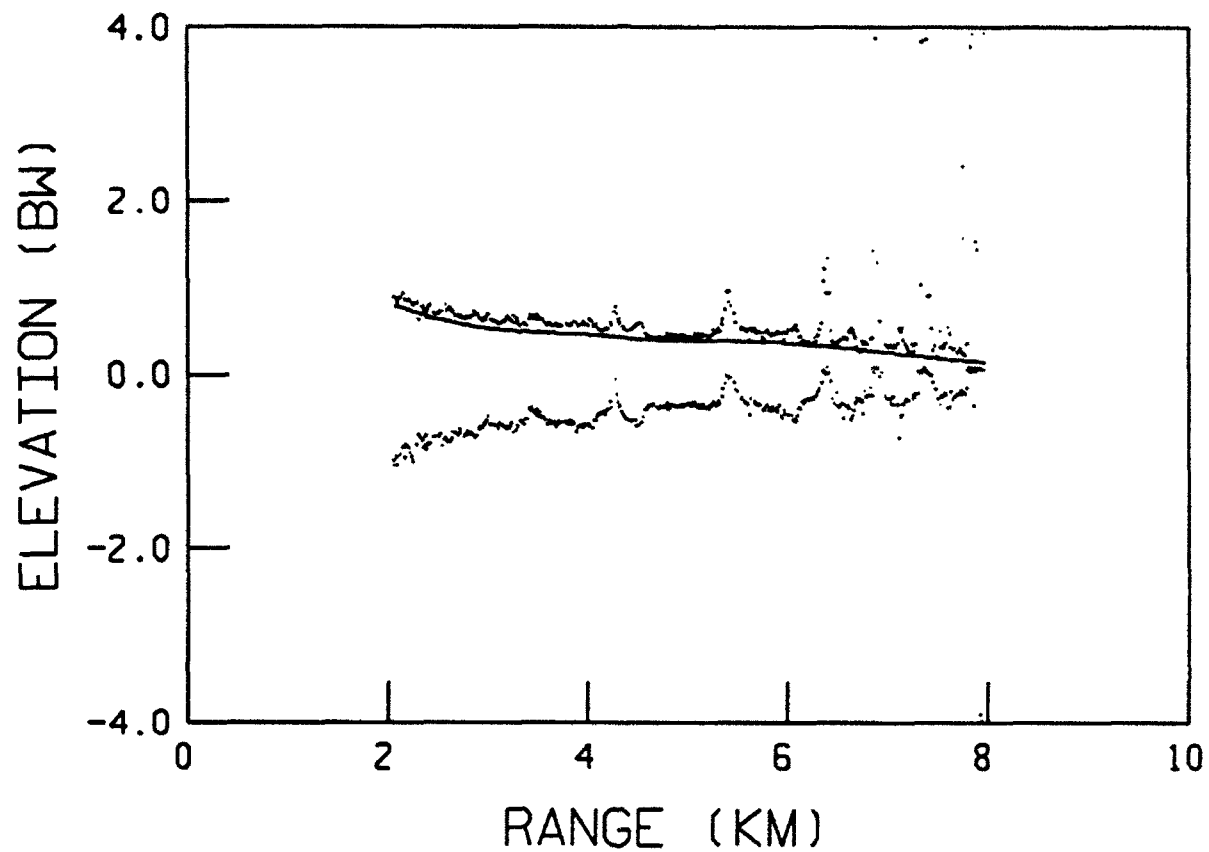


Fig. 4 Signal elevation estimates derived from the fourth STL data file.

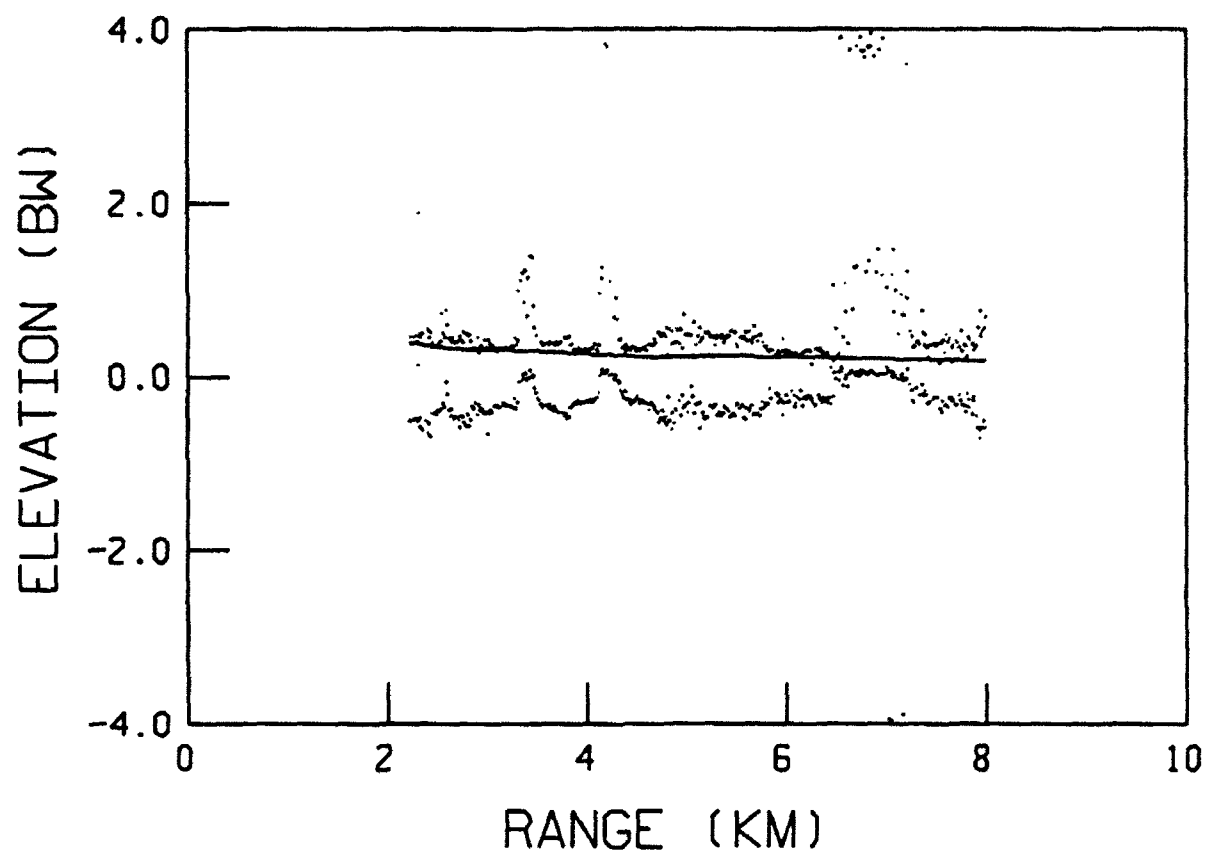


Fig. 5 Signal elevation estimates calculated with the singular value decomposition method and the fifth STL data file.

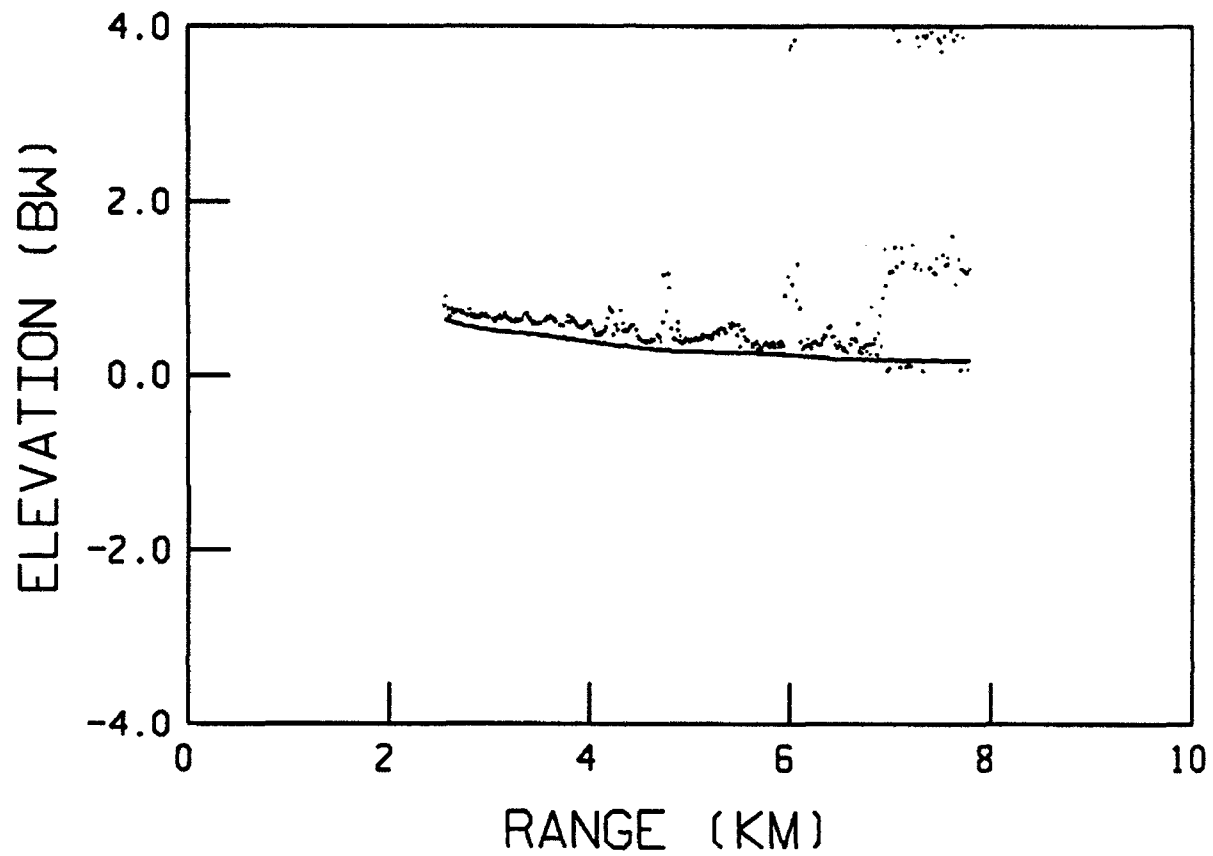


Fig. 6 The larger of the two signal elevation estimates derived from the first STL data file.



#### 4.0 EFFECT OF CALIBRATION PHASE ERRORS ON ELEVATION ESTIMATES

We have studied the effect of calibration phase errors on elevation estimates. The following results are rather general:

- (a) The direction estimates are usually biased. This bias is dependent on the calibration phase errors, and
- (b) The output target and image tracks usually have kinks or branches. The details are also dependent on the calibration phase errors.

Some examples are given in the remainder of this section to illustrate the above observations and to show that calibration phase errors can explain some of the features in Figs. 1 to 5. The antenna and target geometry in the computer simulations are the same as those of the STL experiment on June 18. The reflection coefficient of the water surface is equated to  $-0.794$ , corresponding to 2.0 dB in power attenuation and 180 degrees in phase change. Target signal-to-noise ratio (SNR) at the array elements is modelled to be inversely proportional to the fourth power of range, so that a 50 percent reduction in range leads to a 12 dB increase in SNR. A set of 321 array snapshots are generated as the target range decreases from 10 to 2.0 km. Calibration phase errors, if needed, are those given in the following table.

ELEMENT	PHASE ERROR (DEG)
1	4.769692
2	-2.650831
3	-9.087350
4	-6.525987
5	-5.240850
6	10.306355
7	8.923951
8	-0.494981

Table of calibration phase errors applied to simulated data.

They are defined as

$$\begin{aligned} \text{phase with error} &= \text{phase without error} \\ &+ \text{calibration phase error} . \end{aligned}$$

The average error magnitude in the table is 6.0 degrees, and the largest is about 10.3 degrees. In the convention used, the first array element is the bottom element in the array.

Fig. 7 serves as a reference for comparison. It is obtained by plotting the six candidate signal elevation estimates (because the filter order is given by  $K=6$ ) calculated with each array snapshot and the SVD method. Calibration phase errors are not applied to the data, and the SNR is 26 dB when the target range is 10 km. The estimates produce six tracks: a target track close to and above the zero beamwidth elevation, an image track close to and below the zero beamwidth elevation, and four false tracks with approximately constant elevations at -3.0, -1.8, 1.8, and 3.0 beamwidths.

The false tracks in the above figure can be removed by plotting only the two strongest estimates obtained from each array snapshot. Not visually observable in the figure is the bias in direction estimates. This bias makes the target and image elevation estimates larger than the correct values by an average of about 0.038 degree, or 0.02 beamwidth.

Fig. 8 is obtained by applying the calibration phase errors in Table 1 to the data. As the target range decreases, the lowest false track moves up to the position of the next lowest false track, which in turn moves up to the position of the image track, and so on. This upward movement eventually stops, and kinks appear in the output target and image tracks. The amplitudes of the kinks decrease with the target range.

Fig. 9 is obtained by reversing the signs of the calibration phase errors. The tracks move downwards as target range decreases.

Fig. 10 is obtained by reducing the SNR to 6.0 dB at 10 km target range and plotting only the two strongest elevation estimates obtained with each array snapshot. This figure has many of the kinks and track-branching features found in Figs. 1 to 5.

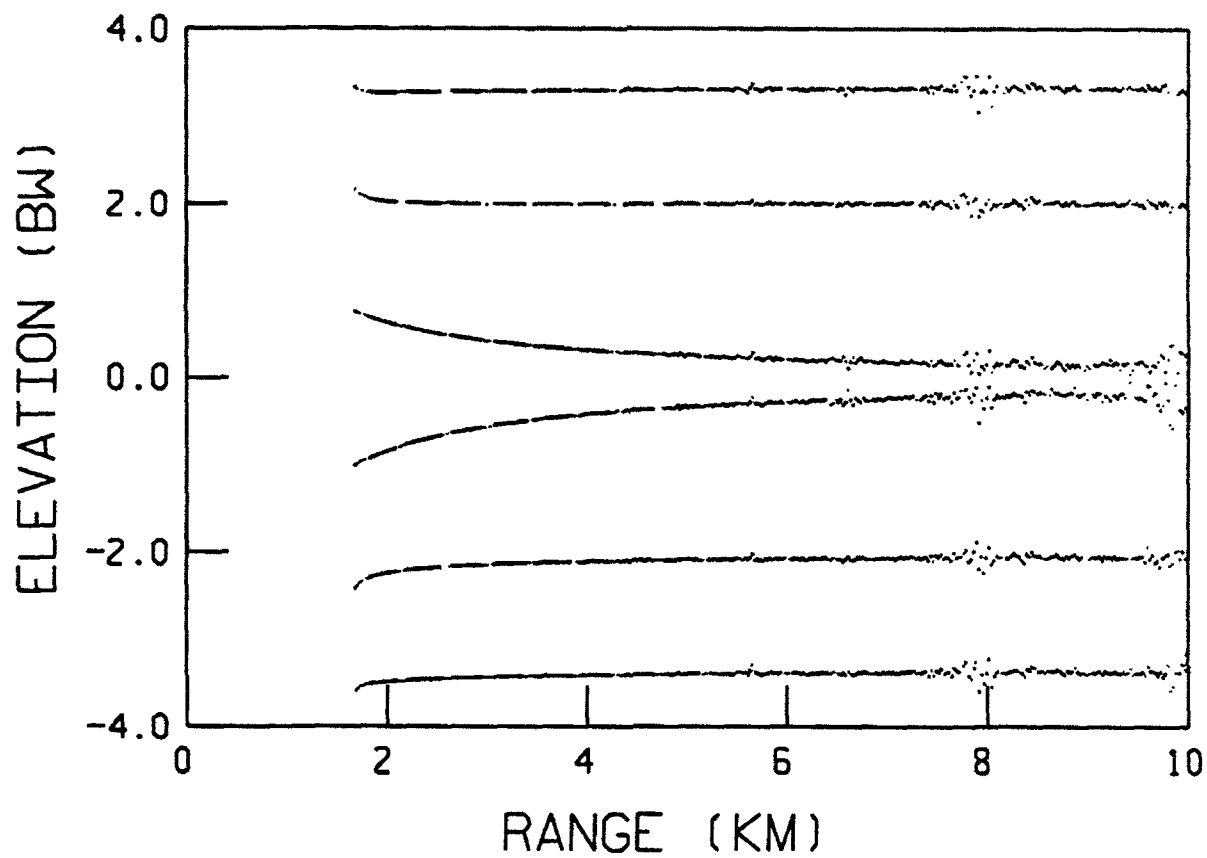


Fig. 7 Candidate signal elevation estimates derived from simulated data. SNR for 10 km target range is 20 dB.

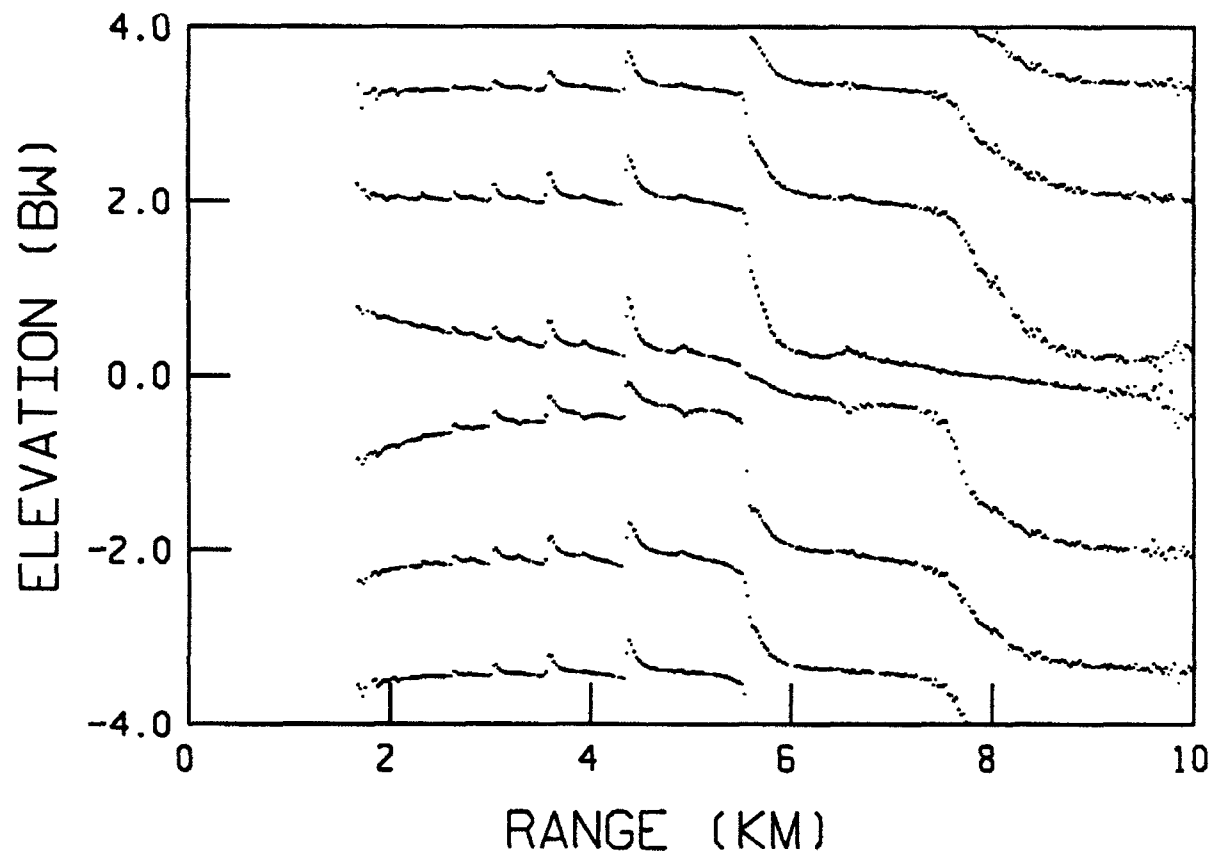


Fig. 8 Candidate signal elevation estimates derived from the simulated data used in Fig. 7. Table 1 for calibration phase errors applied.

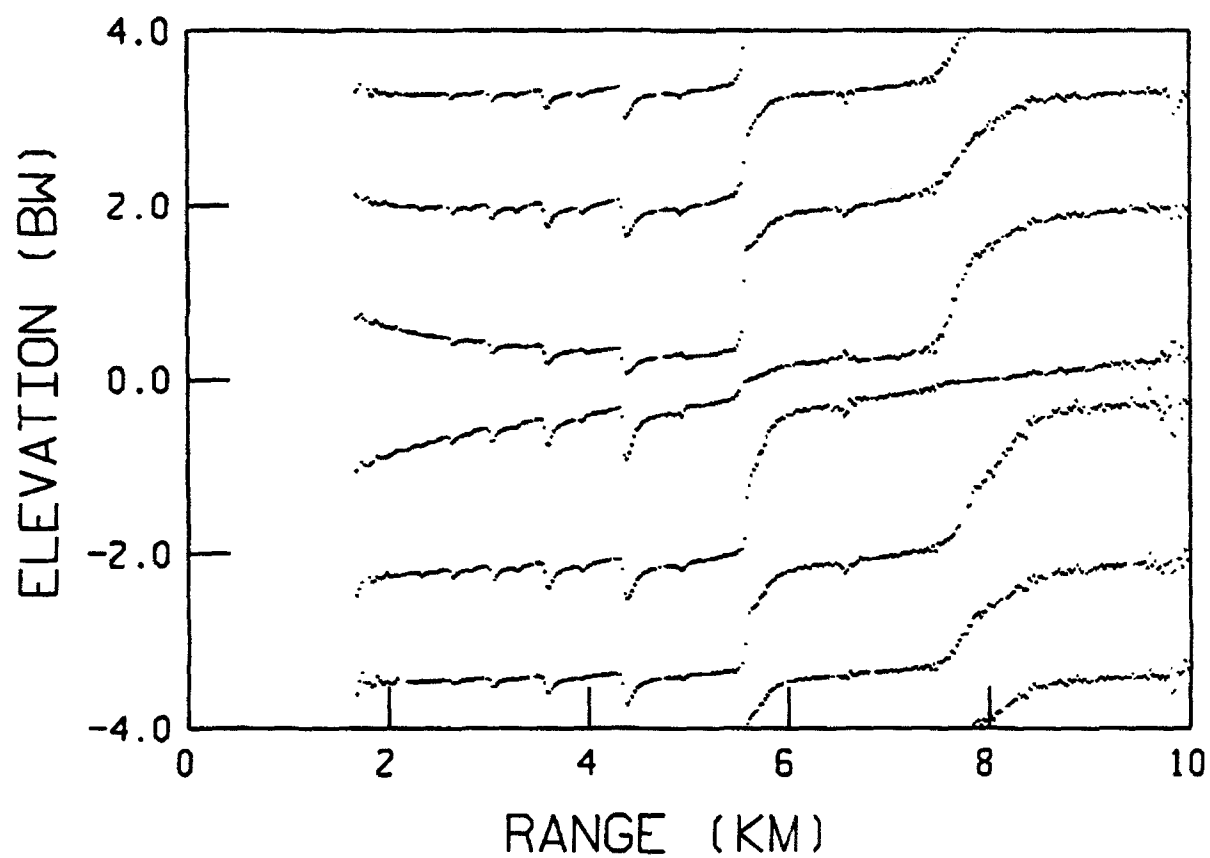


Fig. 9 Candidate signal elevation estimates derived from the simulated data used in Fig. 7. The calibration phase errors are the negative of those in Table 1.

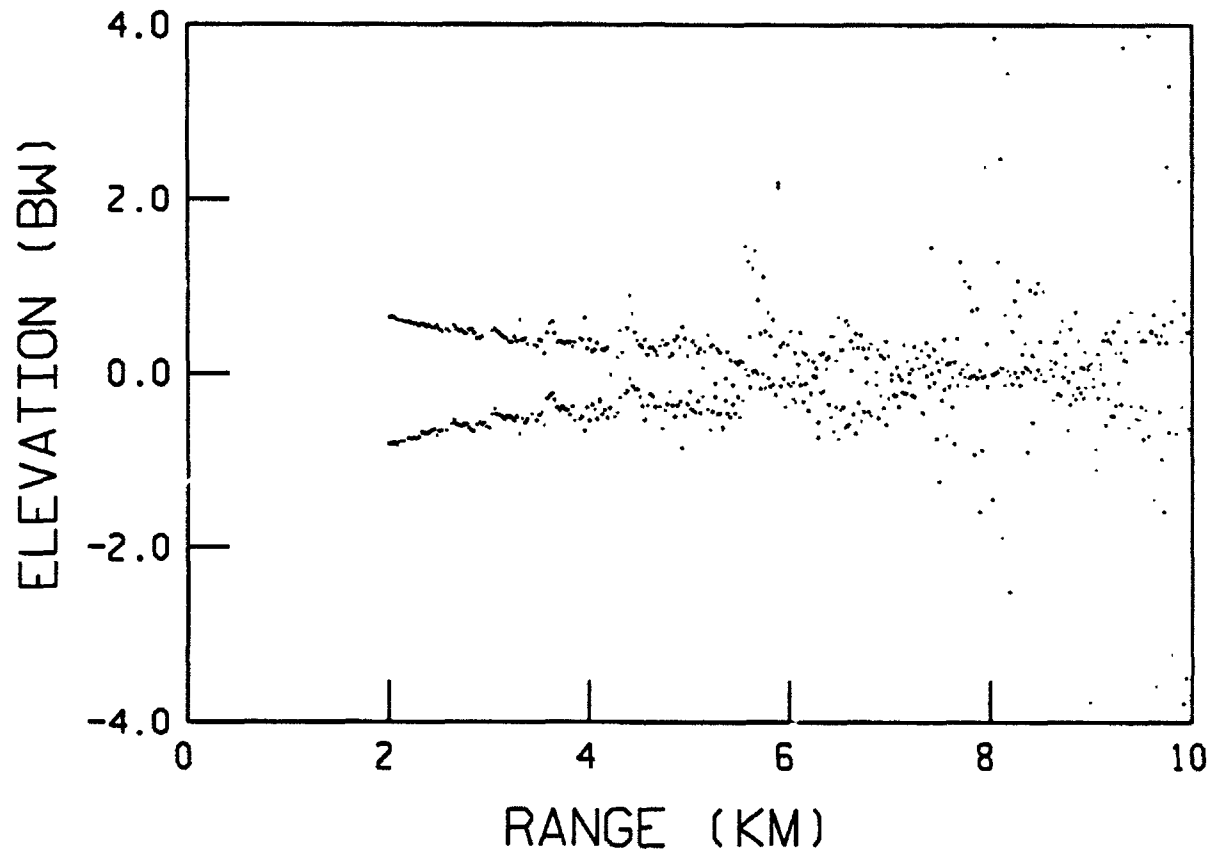


Fig. 10 Signal elevation estimates derived from simulated data. SNR for 10 km target range is 6 dB. Table 1 has been applied to the data.

## 5.0 CONCLUSIONS

We have carried out a new analysis of the multipath radar data measured by STL and observed two new results. Firstly, we can get a target elevation estimate from an array snapshot without using the optical tracker output, if the target range was less than 6.5 km. The procedure is to calculate a set of six candidate signal elevation estimates with the SVD method, find the two with the largest power estimate, and then pick the one with a higher elevation. Secondly, many false tracks branch out from the target and image tracks. Tracks with similar properties can be generated by adding antenna calibration phase errors to uncorrupted simulated data.

The presence of false tracks branching out from the target and image tracks indicates that accurate measurement of the calibration phases of a low-angle tracking array antenna is crucial when the SVD method is used and the array antenna has a small number of elements. Otherwise, long-range data may produce misleading results on target manoeuvres. For example, a horizontally flying target may be wrongly interpreted as a target flying upwards.

### ACKNOWLEDGEMENT

The authors would like to thank the Admiralty Research Establishment and the Standard Telecommunication Laboratories of the United Kingdom for providing the low-altitude tracking data in this study.



## REFERENCES

1. Pearson, A., and W.D. Waddoup, 'Development and Testing of an Array Signal Processing Tracking System', Standard Telecommunication Laboratories, United Kingdom, Contract No. NCW 252/1087, 1981.
2. Tufts, D.W., and R. Kumaresan, 'Estimation of Frequencies of Multiple Sinusoids: Making Linear Prediction Perform like Maximum Likelihood', Proceedings of the IEEE, vol 70, pp. 975-989, September 1982.
3. Kumaresan, R., and D.W. Tufts, 'Estimating the Parameters of Exponentially Damped Sinusoids and Pole-Zero Modelling in Noise', IEEE Transactions on Acoustics, Speech, and Signal Processing, vol. ASSP-30, December 1982.
4. Haykin, S, T. Greenlay, and J. Litva, 'Performance Evaluation of the Modified FBLP Method for Angle of Arrival Estimation using Real Radar Multipath Data', IEE Proceedings, Part F, vol. 132, pp. 159-174, June 1985.

## APPENDIX

### CALCULATION OF ELEVATION ESTIMATES

Presented are the calculations of candidate signal elevation estimates and signal elevation estimates. There are three sections. The first contains the notations and signal model used; the second, the method for calculating a set of K candidate elevation estimates from an array snapshot; and the third, the culling of M signal elevation estimates from the set of K candidate signal elevation estimates.

#### A.1 Notations and Signal Model

The array elements are labelled  $n=1$  to  $N$ , with the first element at the bottom. An array snapshot is denoted by vector  $\mathbf{y}$ , where  $\mathbf{y}=(y_1, y_2, \dots, y_N)^T$  and  $y_n$  is the output of the  $n$ -th array element. Superscript  $T$  denotes the transpose. An array steering vector for elevation  $\phi$  is denoted by

$$\mathbf{v}(\phi) = z^{-0.5(N-1)}(1, z, z^2, \dots, z^{N-1})^T, \quad (\text{A.1})$$

where

$$z = \exp[j2\pi d \sin \phi], \quad (\text{A.2})$$

and  $d$  is the array element spacing in wavelengths.

The signal model is

$$\mathbf{y} = \mathbf{V} \mathbf{a} + \boldsymbol{\eta}, \quad (\text{A.3})$$

where

$$\mathbf{V} = (\mathbf{v}(\phi_1), \mathbf{v}(\phi_2), \dots, \mathbf{v}(\phi_K))^T \quad (\text{A.4})$$

is an  $N \times K$  matrix of array steering vectors,  $K$  is the number of signals,  $\{\phi_1, \phi_2, \dots, \phi_K\}$  are the signal directions,

$$\mathbf{a} = (a_1, a_2, \dots, a_K)^T \quad (\text{A.5})$$

is a vector for the complex signal amplitudes at the array centre, and  $\boldsymbol{\eta}$  is the noise amplitude.

Estimates of the complex signal amplitudes are calculated with (A.3), which gives

$$\hat{\mathbf{a}} = (\mathbf{V}^H \mathbf{V})^\# \mathbf{V}^H \mathbf{y} , \quad (\text{A.6})$$

where superscripts H and # denote the Hermitian-transpose and the Moore-Penrose pseudoinverse, respectively.

## A.2 Computation of Candidate Elevation Estimates

There are three steps in the calculation of candidate elevation estimates.

### Step 1.

Calculate a set of K filter coefficients with the SVD method. Denote them by  $\{g_1, g_2, \dots, g_K\}$ .

### Step 2.

Construct a polynomial as

$$F(z) = 1 + g_1 z^{-1} + g_2 z^{-2} + \dots + g_K z^{-K} . \quad (\text{A.7})$$

### Step 3.

Find the K complex roots of  $F(z)$ , identify them as  $\{z_1, z_2, \dots, z_K\}$ , and calculate the candidate elevation estimates with the relation

$$\arg(z_k) = 2\pi d \sin \phi_k , \quad k=1, 2, \dots, K , \quad (\text{A.8})$$

where  $z_k$  is the k-th root of  $F(z)$  and  $\arg(z)$  is the phase of  $z_k$  in radians.

## A.3 Culling of Signal Elevation Estimates

The M signal elevation estimates are defined as the M candidate signal elevation estimates with the largest power estimates. The power estimates are calculated with (A.6) in three steps.

### Step 1.

Find the eigenvalues and eigenvector of the K by K matrix product  $\mathbf{V}^H \mathbf{V}$ . Arrange them in the order of decreasing eigenvalues. Denote them by  $\{\mu_1, \mu_2, \dots, \mu_K\}$  and  $\{\mathbf{u}_1, \mathbf{u}_2, \dots, \mathbf{u}_K\}$ , respectively.

### Step 2.

Calculate the pseudoinverse of  $\mathbf{V}^H \mathbf{V}$  as

$$(\mathbf{V}^H \mathbf{V})^{\#} = \sum_{k=1}^K \mu_k^{-1} \mathbf{u}_k \mathbf{u}_k^H \quad (\text{A.9})$$

The prime in the summation indicates that only the terms with eigenvalues larger than  $10^{-5}\mu_1$  are included.

### Step 3

- (a) Calculate vector  $\hat{\mathbf{a}}$  with (A.6).
- (b) For  $k=1$  to  $K$ , calculate the power associate with candidate elevation estimate  $\phi_k$  from the components of  $\hat{\mathbf{a}}$  as  $|\hat{a}_k|^2$ .
- (c) Identify the  $M$  candidate elevation estimates with the largest power as the desired  $M$  signal elevation estimates.

The choice of the threshold value, i.e.  $10^{-5}\mu_1$ , in Step 2 is based on the results of a separate study which indicate that the best target and image tracks are obtained if this value is used to process the STL data.

SECURITY CLASSIFICATION OF FORM  
(highest classification of Title, Abstract, Keywords)

## DOCUMENT CONTROL DATA

(Security classification of title, body of abstract and indexing annotation must be entered when the overall document is classified)

1. ORIGINATOR (the name and address of the organization preparing the document. Organizations for whom the document was prepared, e.g. Establishment sponsoring a contractor's report, or tasking agency, are entered in section 8.) National Defence Defence Research Establishment Ottawa Shirley's Bay, Ottawa, Ontario, Canada K1A 0K2		2. SECURITY CLASSIFICATION (overall security classification of the document including special warning terms if applicable)  UNCLASSIFIED	
3. TITLE (the complete document title as indicated on the title page. Its classification should be indicated by the appropriate abbreviation (S,C or U) in parentheses after the title.) A New Analysis of the Multipath Radar Data Measured by Standard Telecommunication Laboratories (U)			
4. AUTHORS (Last name, first name, middle initial) Hung, Eric K.L. Herring, Robert W. Morris, Janet E.			
5. DATE OF PUBLICATION (month and year of publication of document)		6a. NO. OF PAGES (total containing information. Include Annexes, Appendices, etc.) 27	6b. NO. OF REFS (total cited in document) 4
7. DESCRIPTIVE NOTES (the category of the document, e.g. technical report, technical note or memorandum. If appropriate, enter the type of report, e.g. interim, progress, summary, annual or final. Give the inclusive dates when a specific reporting period is covered.)  Technical Report			
8. SPONSORING ACTIVITY (the name of the department project office or laboratory sponsoring the research and development. Include the address.) National Defence Defence Research Establishment Ottawa Shirley's Bay, Ottawa, Ontario, Canada K1A 0K2			
9a. PROJECT OR GRANT NO. (if appropriate, the applicable research and development project or grant number under which the document was written. Please specify whether project or grant) 041LC		9b. CONTRACT NO. (if appropriate, the applicable number under which the document was written)	
10a. ORIGINATOR'S DOCUMENT NUMBER (the official document number by which the document is identified by the originating activity. This number must be unique to this document.)  DREO REPORT 1138		10b. OTHER DOCUMENT NOS. (Any other numbers which may be assigned this document either by the originator or by the sponsor)	
11. DOCUMENT AVAILABILITY (any limitations on further dissemination of the document, other than those imposed by security classification) (X) Unlimited distribution ( ) Distribution limited to defence departments and defence contractors; further distribution only as approved ( ) Distribution limited to defence departments and Canadian defence contractors; further distribution only as approved ( ) Distribution limited to government departments and agencies; further distribution only as approved ( ) Distribution limited to defence departments; further distribution only as approved ( ) Other (please specify):			
12. DOCUMENT ANNOUNCEMENT (any limitation to the bibliographic announcement of this document. This will normally correspond to the Document Availability (11). However, where further distribution (beyond the audience specified in 11) is possible, a wider announcement audience may be selected.)			

UNCLASSIFIED

SECURITY CLASSIFICATION OF FORM

13. **ABSTRACT** (a brief and factual summary of the document. It may also appear elsewhere in the body of the document itself. It is highly desirable that the abstract of classified documents be unclassified. Each paragraph of the abstract shall begin with an indication of the security classification of the information in the paragraph (unless the document itself is unclassified) represented as (S), (C), or (U). It is not necessary to include here abstracts in both official languages unless the text is bilingual).

(U) Presented is a new analysis of some multipath radar data measured with an array antenna and low-flying aircraft by Standard Telecommunication Laboratories (STL) Ltd. The data have previously been analyzed with the singular value decomposition (SVD) method by Haykin, Greenlay, and Litva. These authors were mainly interested in whether or not the SVD method produced elevation estimates consistently close to the true target elevations derived from an adjacent optical tracker. The new analysis, also using the SVD method, has produced additional results. Firstly, it demonstrates a practical technique for selecting target elevation estimates when the target range was less than 6.5 km. Secondly, it provides an explanation, supported with simulations, for the presence of many false tracks branching out from the target and image tracks.

14. **KEYWORDS, DESCRIPTORS or IDENTIFIERS** (technically meaningful terms or short phrases that characterize a document and could be helpful in cataloguing the document. They should be selected so that no security classification is required. Identifiers, such as equipment model designation, trade name, military project code name, geographic location may also be included. If possible keywords should be selected from a published thesaurus, e.g. Thesaurus of Engineering and Scientific Terms (TEST) and that thesaurus-identified. If it is not possible to select indexing terms which are Unclassified, the classification of each should be indicated as with the title.)

Anylysis  
Multipath Radar Data  
Singular Value Decomposition  
Calibration Phase Errors

UNCLASSIFIED

SECURITY CLASSIFICATION OF FORM